Biomaterials 32 (2011) 3072–3084

Contents lists available at ScienceDirect

Biomaterials

journal homepage: www.elsevier.com/locate/biomaterials

Flotillin-dependent endocytosis and a phagocytosis-like mechanism for cellular internalization of disulfide-based poly(amido amine)/DNA polyplexes☆

Dries Vercauteren [a], Martin Piest [b], Leonardus J. van der Aa [b], Monerah Al Soraj [c], Arwyn T. Jones [c], Johan F.J. Engbersen [b], Stefaan C. De Smedt [a], Kevin Braeckmans [a,*]

[a] Laboratory of General Biochemistry and Physical Pharmacy, Ghent University, Harelbekestraat 72, B-9000 Ghent, Belgium
[b] Department of Biomedical Chemistry, MIRA Institute for Biomedical Technology and Technical Medicine, Faculty of Science and Technology, University of Twente, P.O. Box 217, 7500 AE Enschede, The Netherlands
[c] Welsh School of Pharmacy, Redwood Building, Cardiff University, CF10 3NB, Cardiff, Wales, UK

ARTICLE INFO

Article history:
Received 28 October 2010
Accepted 27 December 2010
Available online 22 January 2011

Keywords:
Non-viral gene delivery
Endocytosis
Retinal pigment epithelium
Polyplexes

ABSTRACT

Extensive research is currently performed on designing safe and efficient non-viral carriers for gene delivery. To increase their efficiency, it is essential to have a thorough understanding of the mechanisms involved in cellular attachment, internalization and intracellular processing in target cells. In this work, we studied *in vitro* the cellular dynamics of polyplexes, composed of a newly developed bioreducible poly(amido amine) carrier, formed by polyaddition of *N,N*-cystamine bisacrylamide and 1-amino-4-butanol (p(CBA-ABOL)) on retinal pigment epithelium (RPE) cells, which are attractive targets for ocular gene therapy. We show that these net cationic p(CBA-ABOL)/DNA polyplexes require a charge-mediated attachment to the sulfate groups of cell surface heparan sulfate proteoglycans in order to be efficiently internalized. Secondly, we assessed the involvement of defined endocytic pathways in the internalization of the polyplexes in ARPE-19 cells by using a combination of endocytic inhibitors, RNAi depletion of endocytic proteins and live cell fluorescence colocalization microscopy. We found that the p(CBA-ABOL) polyplexes enter RPE cells both via flotillin-dependent endocytosis and a PAK1 dependent phagocytosis-like mechanism. The capacity of polyplexes to transfect cells was, however, primarily dependent on a flotillin-1-dependent endocytosis pathway.

1. Introduction

Efficient delivery of therapeutic nucleic acids into designated cells and subsequent availability at the intracellular site of action are crucial requirements for successful gene therapy. It is generally accepted that gene carriers are internalized through endocytic vesicles which are then trafficked to other regions of the cell. Thus, the mechanisms that direct cell attachment, endocytosis, intracellular trafficking and release of the nucleic acids from the carrier strongly determine transfection efficiency. Most of these processes are generally dictated by the nature of the gene carrier. It is known that for non-viral gene delivery vehicles both cellular entry and intracellular release of therapeutic nucleic acids is significantly less efficient compared with viral vectors, and non-viral gene therapy thus generally suffers from low transfection efficiencies [1]. They are, however, attractive alternatives to viral carriers, because they are safer to use, are less immunogenic, can be more easily chemically modified and are easier to produce at large-scale. In order to design safe and efficient non-viral carriers for gene delivery, we need a better understanding of the mechanisms involved from cell uptake to intracellular fate. In this respect, cell surface targets need to be identified and evaluated to improve cell attachment and vector internalization to deliver the gene through transfection-efficient pathways. This knowledge will allow further improvements in the design and functionalization of the delivery vehicle with the intention of developing target-specific, effective and safe carriers for nucleic acid delivery.

Currently, the mechanisms behind the cellular processing of non-viral gene complexes remain poorly understood since the highly dynamic character of these processes makes these studies very complex. In addition, the interaction between the target cell and the gene complex might be highly cell-type specific for the type of particle being studied. Therefore, little consistency is found in the scientific literature. The situation is further complicated due to the fact that a single cell can harbor a number of different endocytic pathways and because of interconnections and interdependences between these endocytic processes. However, a common endocytosis classification based on recent reviews distinguishes phagocytosis, macropinocytosis, clathrin-dependent endocytosis (CDE) and

☆ The work is done in Ghent, Belgium.
* Corresponding author. Tel.: +32 (0) 9/2648098; fax: +32 (0) 9/2648189.
E-mail address: kevin.braeckmans@UGent.be (K. Braeckmans).

0142-9612/$ – see front matter © 2011 Elsevier Ltd. All rights reserved.
doi:10.1016/j.biomaterials.2010.12.045

clathrin-independent endocytosis (CIE) [2]. Phagocytosis is characterized by the engulfment of large solid particles of at least 1 μm in size, typically restricted to specialized cells such as macrophages. Macropinocytosis is an induced and transient bulk internalization process, that is typically characterized by the formation of membrane ruffles and the engulfment of large volumes of fluid and membrane into large uncoated vacuoles [3,4]. In addition, some cell types like immature dendritic cells and macrophages exhibit constitutive macropinocytosis, constantly surveying their environment for foreign material [4]. Possibly the best-studied endocytic pathway to date is CDE, which is characterized by the formation of clathrin-coated pits [5]. CIE includes several pathways which all share a dependency on cholesterol [6]. Some of the currently known CIE pathways are caveolin mediated endocytosis (Cav-ME) [7], flotillin mediated endocytosis (Flot-ME) [8], and the pathway clathrin-independent carriers - GPI-enriched endocytic compartments (CLIC/GEEC) [9]. It is clear from recent literature that the use of different endocytic routes is strongly dependent on the cell type, gene carrier and nucleic acid [10–12]. It is also becoming apparent that some endocytic pathways will allow a higher transgene delivery and thus efficiency of transfection than others. For example, polyplex uptake is reported to occur via MP, CDE as well as via CIE [13–15]. And although no consensus yet exists on the description of the exact endocytic pathway that would lead preferentially to transfection, some reports seem to agree that CDE is less preferable for polyplex mediated gene transfer [12,16–18].

Studying endocytic pathways is typically done by attempting to selectively inhibit different endocytic pathways and then quantifying the remaining internalized gene complexes. These studies are often carried out with the help of pharmaceutical endocytic inhibitors [19,20]. However, due to problems of low specificity, alternative methods such as RNA interference (RNAi), transfection of cells with mutant proteins and fluorescence colocalization microscopy have been employed as alternative tools [14]. In this work we have combined these approaches to study endocytosis of a polymeric carrier in retinal pigment epithelium (RPE) cells. These cells form *in vivo* a monolayer of highly specialized cells, interposed between the neurosensory retina and the choroid [21]. This light-absorbing epithelium functions as a blood-retina barrier, regulating the transport of nutrition to the retina [21]. RPE cells are attractive targets for ocular gene therapy because they are involved in several ocular genetic defects such as retinitis pigmentosa and choroidal neovascularization (e.g. AMD) which could conceivably be cured by altering the expression profile in these cells [22,23]. The polymeric vector in this study is p(CBA-ABOL), a linear poly(amido amine) with repetitive disulfide linkages in the main chain, prepared by Michael-type polyaddition of 4-aminobutanol (ABOL) to *N*,*N*′-cystaminebisacrylamide (CBA) [24]. This polymer contains tertiary amines that are partially protonated around physiological pH, which makes the polymer positively charged and suitable to form positively charged polyplexes by electrostatic interaction with anionic nucleic acids. The disulfide bonds in the polymeric backbone are prone to rapid cleavage into sulfhydryl groups once the polymer has arrived in the reductive intracellular environment due to the presence of thioredoxin reductases and high glutathione concentrations. This identifies this polymer as a "bioreducible polymer" that is rapidly degraded in the intracellular milieu, thereby releasing the DNA from the polymer/DNA complex [25].

The purpose of this work was to gain insight into the mechanisms of attachment and internalization of p(CBA-ABOL)/DNA polyplexes in ARPE-19 cells. We initially evaluated the transfection efficacy and uptake kinetics of p(CBA-ABOL) polyplexes in primary RPE cells and ARPE-19 cells and also investigated the attachment of the polyplexes to RPE cells. Secondly, we studied endocytic uptake of p(CBA-ABOL)/DNA polyplexes by using a library of different endocytic inhibitors. Thirdly, as a complementary strategy, we utilized RNAi to downregulate specific proteins that play key roles in endocytic processes to block the corresponding endocytic events. Finally, we performed fluorescence colocalization microscopy studies to confirm association of the polyplexes with endocytic proteins.

2. Materials and methods

2.1. Materials

Heparinase III, trypan blue, Cpz, MβCD, genistein, nocodazole, dynasore, rottlerin, Lucifer Yellow CH dilithium salt (LY), (defatted) bovine serum albumin (BSA) and sodium chlorate were purchased from Sigma–Aldrich (Bornem, Belgium). Dulbecco's modified Eagle's medium (DMEM), OptiMEM, L-glutamine, fetal bovine serum (FBS), penicillin-streptomycin solution (5000 IU/ml penicillin and 5000 μg/ml streptomycin) (P/S), and phosphate-buffered saline (PBS) were supplied by GibcoBRL (Merelbeke, Belgium). CytoD, human Transferrin (hTf)-AlexaFluor488, BSA-complexed BODIPY FL C5-Lactosylceramind (LacCer), Oregon Green labeled 70 kDa dextran and FITC labeled *Escherichia coli* Bioparticles™ (ECs) were purchased from Invitrogen (Merelbeke, Belgium). Sequences of siRNAs and manufacturer are given in Supplementary. Table. 1. Antibodies against heparan sulfate were purchased from Millipore (Brussels, Belgium). Antibodies for Western blotting are listed in Supplementary. Table. 2. JetPEI™ was purchased from Polyplus (Leusden, The Netherlands). Lipofectamin2000™ for gene transfection and LipofectaminRNAiMAX™ for transfection of siRNA were purchased from Invitrogen (Merelbeke, Belgium). All other reagents were purchased from Sigma–Aldrich (Bornem, Belgium) unless otherwise stated.

2.2. Cell culture

ARPE-19 cells (retinal pigment epithelial cell line; ATCC number CRL-2302) were cultured in DMEM:F12 supplemented with 10% FBS, 2 mM L-glutamine, and 2% P/S. All cells were grown at 37 °C in a humidified atmosphere containing 5% CO_2. Primary bovine RPE cells were isolated from fresh bovine eye bulbs and prepared for culture as previously described [81]. Briefly, after cleaning the fresh eyes from fat, muscle and connective tissue, the eye bulb was dissected around the pupil. The lens and vitreous liquid were then removed and the remaining eyecup was washed in PBS with 4% P/S until the retina detached from the underlying RPE and choroid. After removal of the retina, the eyecup was washed twice with 6 ml of 0.25% w/v trypsin and 1 mM EDTA in PBS for 30 min at 37 °C to detach RPE cells from the underlying choroid. The cells were diluted in cell culture media with 20% FBS and after centrifugation they were seeded in 25 cm^2 culture flasks (SPL Life Sciences, Pocheon, Korea). After 24 h of culture, the adherent cells were washed to discard remaining blood cells. Primary bovine RPE cells were used between passages 6 and 10. All cells were grown at 37 °C in a humidified atmosphere containing 5% CO_2.

2.3. Plasmids

The plasmid construct pEGFP-Flot2 was a kind gift from B. Nichols (Cambridge University, UK) and pEGFP-Cav1 was a kind gift from M. Gumbleton (Cardiff University, UK). Plasmids were all transformed in single step (KRX) competent cells (Promega, Leiden, The Netherlands) according to the manufacturer's instructions. The transformed bacteria were then selected for kanamycin resistance and grown to OD of 1.5. The plasmids were isolated with a QIAfilter Plasmid Giga Kit (Qiagen, Venlo, The Netherlands) and concentrations determined by UV absorption at 260 nm. Finally, the plasmids were suspended and stored in 20 mM HEPES, pH 7.4.

For all plasmid uptake studies, pGL4.13 plasmid (Promega, Leiden, The Netherlands), labeled with the nucleic acid stain YOYO-1™ (λ_{ex} = 491 nm, λ_{em} = 509 nm, Molecular Probes, Merelbeke, Belgium) was used. This is a 4641 base pair (bp) construct and contains a luciferase 2 expression cassette under control of the cytomegalovirus (CMV) promoter, next to a sequence for ampicillin resistance. YOYO-1 (1 mM in DMSO) iodide was added to the plasmid at a mixing ratio of 0.15:1 (v:w) ratio of (dye/base pair), resulting in a theoretical labeling density of 1 YOYO-dye molecule per 10 bp. The mixture was incubated at room temperature for 1 h in the dark. To remove the DMSO and free YOYO-1, the complex was precipitated adding 2 volumes of ice-cold ethanol and 0,1 volume of 5 M NaCl. After incubation for 30 min at 4 °C, centrifugation (17.000 g, 10 min) and washing with ice-cold 70% ethanol, fluorescently labeled plasmid was finally resuspended in 25 mM HEPES, pH 7.2. The concentration of the plasmid was again determined by UV absorption at 260 nm. For microscopy colocalization studies with GFP labeled structures, pGL4.13 plasmid was labeled with Cy5 (Label IT Nucleic Acid Labeling Kit, Mirus Bio Corporation, WI, USA), according to the manufacturer's instructions at a 1:2 (v:w) ratio of Label IT Tracker Reagent and plasmid. For all transfection studies, gWiz™-GFP plasmid (Aldevron, Freiburg, Germany) was used, consisting of 5757 bp and containing the GFP expression cassette under control of the CMV promoter, next to CMV introns and kanamycin resistance.

2.4. Polyplexes

p(CBA-ABOL)/DNA complexes were obtained by adding a polymer solution of 0.6 mg/ml to a plasmid solution of 0.05 mg/ml in a final mass ratio of 48/1 in 25 mM HEPES buffer pH 7.2 and vortexing the mixture for 10 s. These gene complexes have an average hydrodynamic diameter of 120 nm and an average zeta potential of +40 mV (See Supplementary. Fig. 3). This was measured in undiluted samples of the polyplexes on a NanoZS zetasizer (Malvern Instruments, Hoeilaart, Belgium). For every transfection, fresh polyplexes were made and used within 30 min after complexation and were diluted 5× in OptiMEM™ during the addition to the cells.

JetPEI polyplexes were prepared according to the manufacturer's instructions. In summary, 4 μg of pDNA and 8 μl of JetPEI were first separately diluted till 100 μl with a 150 mM NaCl solution. The JetPEI dilution was then added to the pDNA solution, shortly vortexed and used within 30 min after the mixing step. Before adding the polyplexes to the cells, the polyplexes were first diluted 10× in OptiMEM™.

2.5. Pretreatments with pharmacological endocytic inhibitors

For all inhibition studies, 2×10^5 cells were seeded in six-well plates to, 24 h later, reach 70% confluency. The cells were subsequently pre-incubated with endocytic inhibitor in OptiMEM™ 15 μg/ml Cpz, 400 μM genistein and 3 mM MβCD for 2 h, 10 μM rottlerin, 5 μg/ml nocodazole and 5 μg/ml CytoD for 1 h or 80 μM dynasore for 30 min. All endocytic inhibitors were freshly used and fresh inhibitor was also added during uptake period with fluorescently labeled endocytic markers or polyplexes. MβCD and chlorpromazine solutions were filter sterilized through a 0.22 μm pore size filter before use.

2.6. siRNA mediated depletion of endocytic proteins

Cells were seeded at 2×10^5 cells per well in six-well plates and 24 h later transfected with 150 pmol siRNA (See Supplementary. Table. 1) and 7 μl LipofectaminRNAiMAX™ per well in serum free OptiMEM™ for 4 h according to the manufacturer's instructions. As a negative control, cells were transfected with Negative Control siRNA (Eurogentec, Seraing, Belgium) (Supplementary. Table. 1). Cells were subsequently left in growth medium for 20 h before detachment with trypsin and seeding them in 75 cm^2 culture flasks. After another 24 h, cells were transfected for a second time in the culture flask with 1.25 nmol siRNA and 58 μl LipofectaminRNAiMAX™ in OptiMEM™ for 4 h. After 20 h, cells were detached again and seeded in six-well plates in full growth medium and incubated for 12 h before performing endocytosis and transfection assays or cell lysis for assessing depletion (below).

2.7. Immunodetection of proteins following siRNA depletion

Following transfection with siRNA, the cells were washed and incubated for 5–10 min with ice-cold lysis buffer (50 mM Tris-base, 150 mM NaCl, pH 8.0, 1% Triton X-100) containing protease inhibitor cocktail (Roche, Vilvoorde, Belgium). The lysate was centrifuged at 13,000*g* (4 °C) for 10 min and supernatants were collected for protein analysis with the BCA protein assay kit (Pierce, Erembodegem, Belgium). Then, 20 μg protein was resolved by SDS-PAGE and transferred to nitrocellulose membranes, which were then blocked for 45 min at RT with (TBS containing 5% dried skimmed milk) then probed with CHC, Flot1, Cav1, DNM2, GRAF1, ARF6 and PAK1 antibodies (Supplementary. Table. 2), washed and then incubated with horseradish peroxidase-conjugated anti mouse, anti-rabbit or anti-goat antibodies (Pierce, Northumberland, UK). Protein bands were visualized by the enhanced chemiluminescence detection system (Thermo Fisher, Scientific, Leicestershire, UK). Equal protein loading was confirmed using antibodies recognizing α-Tubulin or CHC.

2.8. Flow cytometry

Cell-associated fluorescence was analyzed with a 5-color FACS Calibur (Beckton Dickinson, Erembodegem, Belgium) equipped with an Argon laser (excitation 488 nm) and a red diode laser (excitation 635 nm). For quantification, all experiments were performed in triplicate and for each sample 1×10^4 events were collected by list-mode data that consisted of side scatter, forward scatter and fluorescence intensities in different channels. Fluorescence emission of AF488, Oregon Green, LY, FITC and Bodipy FL was detected with a 530/30 nm bandpass filter (FL1) and emission of trypan blue was detected with a 670 long pass filter (FL4). Cellquest software (Beckton Dickinson, Erembodegem, Belgium) was used for analysis. Appropriate gating was applied to the scatterplot of untreated cells to select for intact cells. FL1 and FL4 signals were measured for all gated cells.

2.9. Quantification of uptake of endocytic markers or polyplexes

Control or inhibitor pre-treated cells, seeded 24 h earlier in six-well plates at 2×10^5 cells per well, were incubated with fluorescently labeled endocytic marker or gene complexes in OptiMEM™. Due to the presence of hTf in OptiMEM, DMEM was used as an alternative hTf free medium. The concentration and incubation time for the different endocytic markers were applied under following conditions: 16.7 μg/ml hTf for 15 min, 0.81 μM LacCer for 15 min, 5 mg/ml LY for 1 h, 0.5 mg/ml 70 kDa dextran for 3 h and 0.2 mg/ml ECs for 3 h. Polyplexes of p(CBA-ABOL) and YOYO-1 labeled pGL4.13 were incubated with the cells for 2 h at an amount corresponding to 4 μg plasmid per well. For quantification of the internalized fraction of endocytic marker or gene complexes with flow cytometry, it is imperative to remove the fraction that was not internalized and is still associated with the plasma membrane. For hTF and LacCer we applied an acid wash and back exchange protocol, respectively, as described previously [19]. The fluorescence of the plasma membrane associated fraction of FITC labeled ECs, Oregon Green labeled dextran, LY or YOYO-1 labeled pDNA was quenched with a 0.2% trypan blue solution in PBS for 5 min at room temperature. After thorough washing steps with PBS, cells were detached with trypsin, centrifuged and resuspended in ice-cold PBS with 0.1% azide and 1% BSA. Mean fluorescence values of triplicates were analyzed with flow cytometry and used as a measure for uptake of the endocytic markers or gene complexes. For inhibition experiments, mean fluorescence values were corrected for a 0% uptake (negative control) and normalized to a 100% uptake (positive control). The 0% uptake was determined from cells which were incubated with the fluorescent endocytic markers or complexes at 4 °C and underwent the same acid wash, back exchange or quenching. Uptake corresponding to 100% was determined from cells which were not treated with any inhibitor or with control siRNA.

2.10. Analysis of transfection efficiency

Cells were seeded into 6-well plates (2×10^5 cells per well) and allowed to attach overnight. Subsequently, the culture medium was removed and gene complexes, composed of gWiz™-GFP pDNA and gene carrier, were added to the well (4 μg of DNA per well). After 2 h, cells were washed with PBS and incubated for 22 h in full cell culture medium, unless stated differently. The average GFP expression of the total gated population of cells and the amount of GFP-positive cells in the same gate were subsequently measured by flow cytometry. As a negative control, cells were transfected with pGL4.13 plasmid since luciferase expression does not produce a detectable signal in the FL1 channel of the flow cytometer. A cell was considered GFP-positive and therefore successfully transfected if the average fluorescence was above the threshold *T*, defined as the 99.5 percentile of the negative control sample. For inhibition experiments, GFP values were corrected for negative control (0% transfection) and normalized to the positive control (100% transfection), the latter being cells that were not treated with any inhibitor or with control siRNA.

2.11. Fluorescence colocalization microscopy

ARPE-19 cells were seeded at a concentration of 300.000 cells per well on sterile MatTek coverslips (1.5)-bottom dishes (MatTek Corporation, MA, USA). The next day, cells were transfected with plasmids coding for the EGFP constructs (pEGFP-Flot2 and pEGFP-Cav1) using Lipofectamin2000™ (Invitrogen, Merelbeke, Belgium) according to the manufacturer's description. The staining with pEGFP-Flot1 not satisfactory, and therefore omitted in this study. Briefly, for every Petri dish, 7 μl of Lipofectamin2000™ was mixed with 4 μg plasmid in 500 μl OptiMEM™ and after 30 min, these lipoplexes were added to 1500 μl OptiMEM™ on top of the cells. After 4 h, the lipoplex containing medium was removed and replaced with full cell culture medium. 24 hr later, the cells were incubated with p(CBA-ABOL) polyplexes, 5× diluted in 2 ml OptiMEM™, representing 4 μg Cy5-labeled pGL4.13 plasmid per well. Mixing the polyplexes with OptiMEM™ induces the formation of micrometer sized polyplex aggregates. Therefore, after 15 min, polyplexes were washed away and replaced with cell culture medium to reduce the amount of bright, non-internalized polyplex aggregates that can cause high background intensity in the fluorescence images. Cells were finally placed in a stage top incubation chamber (Tokai Hit, Shizuoka, Japan), on the microscope, set at 37 °C, 5% CO_2 and 100% humidity. GFP transfected cells were chosen for imaging based on a relatively low expression level of GFP-constructs. Cells were imaged on a custom built wide field fluorescence microscope set-up using a TE2000-E inverted microscope equipped with a Plan Apo VC 100× 1.4 NA oil immersion objective lens (Nikon Belux, Brussels, Belgium). GFP was excited with a 491 nm laser line (Cobolt, Stockholm, Sweden), while Cy5 was excited with a 636 nm diode laser (IQ1C, Power Technology, Little Rock, AR). GFP emission was captured in a spectral range between 500 and 600 nm and Cy5 between 655 and 745 nm. GFP and Cy5 fluorescence images were registered simultaneously on separate halves of the chip of an EMCCD camera (Roper Scientific, Nieuwegein, The Netherlands) and the overlay of the two channels was obtained with custom developed software.

3. Results

3.1. In vitro evaluation of p(CBA-ABOL) as a carrier for gene delivery

Linear disulfide-containing poly(amido amine) polymers such as p(CBA-ABOL) are promising carriers for nucleic acid delivery as disulfide-containing polymers have shown to offer higher average transgene expression and lower cytotoxicity, compared to polyethylenimine (PEI) which is typically considered as the standard

reference for polymer based gene delivery [24,26–29]. To evaluate the transfection efficiency of p(CBA-ABOL) in RPE cells, we compared transgene expression of p(CBA-ABOL) polyplexes with commercially available linear PEI vector JetPEI™ and the lipid based transfection agent Lipofectamin2000™. This was done both in ARPE-19 cells, a continuous human cell line of the RPE, as well as in primary bovine RPE cells (BRPE). RPE cells were transfected in serum free OptiMEM™ for 2 h with 4 μg of gWiz™-GFP plasmid, complexed with the different carriers. The percentage of GFP-positive cells and the average GFP expression were determined by flow cytometry, 24 h post-transfection (Fig. 1). This time point was chosen, because analysis of GFP expression for up to 5 days after transfection in ARPE-19 cells with p(CBA-ABOL) polyplexes showed that maximum GFP expression is reached after 24 h (Supplementary. Fig. 1). In the case of ARPE-19 cells, p(CBA-ABOL) polyplexes were able to transfect 80% of the cell population (Fig. 1, black dots), which was similar to Lipofectamin2000™ lipoplexes, but significantly higher than JetPEI™. Similar observations were obtained for average GFP expression (Fig. 1, black bars).

To further assess the transfection capacity of p(CBA-ABOL) complexes, we also performed experiments on primary bovine RPE cells. Similar trends were observed, although the percentage of transfected cells and average GFP expression was consistently less, compared to ARPE-19 cells. In addition, we assessed immediate cytotoxicity in ARPE-19 cells of the p(CBA-ABOL) transfection for different p(CBA-ABOL)/DNA mass ratios (Supplementary. Fig. 2). Higher mass ratios generally resulted in higher transfection efficiencies, but these were also more toxic to the cells [24]. As a trade off, a mass ratio of 48/1 was chosen for all further experiments since this ratio did not cause any significant cytotoxicity after 2 h exposure to the cells (Supplementary. Fig. 2), while still saturating the cellular uptake machinery (Supplementary. Fig. 3) and leading to high transfection efficiencies (Fig. 1). From these experiments we conclude that under defined conditions p(CBA-ABOL) is a safe and highly efficient polymeric carrier for DNA delivery to the RPE.

3.2. Role of anionic cell surface proteoglycans in p(CBA-ABOL) polyplex attachment and internalization

In order to study the interaction of p(CBA-ABOL)/DNA polyplexes with the plasma membrane, we investigated the role of highly anionic cell surface heparan sulfate proteoglycans (HSPGs). Cell surface HSPGs make up a great deal of the extracellular matrix (ECM) of different cell types [30] and it is known that they can function as primary co-receptors for cellular entry of lipoproteins [31], pathogenic bacteria, cell penetrating peptides [32], viruses [33] and also non-viral gene complexes [14,34,35]. For this reason, we investigated the role of HSPGs in attachment and subsequent uptake of p(CBA-ABOL) polyplexes in ARPE-19 cells. First, we attempted to interfere with the charge interaction between the cationic polyplexes and anionic HSPG chains by adding exogenous heparan sulfate analogs [31]. For this, ARPE-19 cells were exposed for 2 h to YOYO-1 labeled p(CBA-ABOL) polyplexes in OptiMEM in the presence of 10 mg/ml heparin. The presence of heparin led to an increase in size of the polyplexes and caused a charge reversal of the polyplexes to −60 mV (See also Supplementary. Fig. 4). After this 2 h exposure, the cells were washed and the fluorescence of the membrane bound fraction of polyplexes was quenched with trypan blue. Interestingly, since trypan blue formed complexes with the non-internalized polyplexes during the quenching step, trypan blue fluorescence could be used as a measure of plasma membrane associated polyplexes, or in other words cellular attachment. Both cellular attachment (Fig. 2, black bars) and endocytosis (Fig. 2, gray bars) of the p(CBA-ABOL) polyplexes were quantified by flow cytometry. The presence of heparin and consequent charge reversal of the polyplexes completely blocked cellular adhesion and uptake of the polyplexes (Fig. 2). This highlights the charge-based nature of the interaction between p(CBA-ABOL) polyplexes and the cell surface. We note that similar effects were observed when incubating the polyplexes in the presence of 10% FBS, probably because of similar binding of the abundant serum protein albumin and other proteins to the polyplexes (data not shown).

In a complementary experiment, we attempted to interfere with cellular sulfation by inhibiting ATP-sulfurylase, the enzyme that maintains the cellular sulfate pool. Here, ARPE-19 cells were pre-treated for 24 h with 80 mM of sodium chlorate as this treatment is reported to result in a strong reduction of the sulfation of the HSPGs (Keller, 1989). Sodium chlorate treated cells were then incubated with YOYO-1 labeled p(CBA-ABOL) polyplexes and their cell attachment and uptake were measured after 2 h. As a control experiment, uptake of hTf and LY after chlorate treatment was also assessed. hTf is specifically internalized via CDE after binding to the transferrin receptor [5] and LY, a small anionic hydrophilic membrane impermeable fluorescent molecule, is internalized via

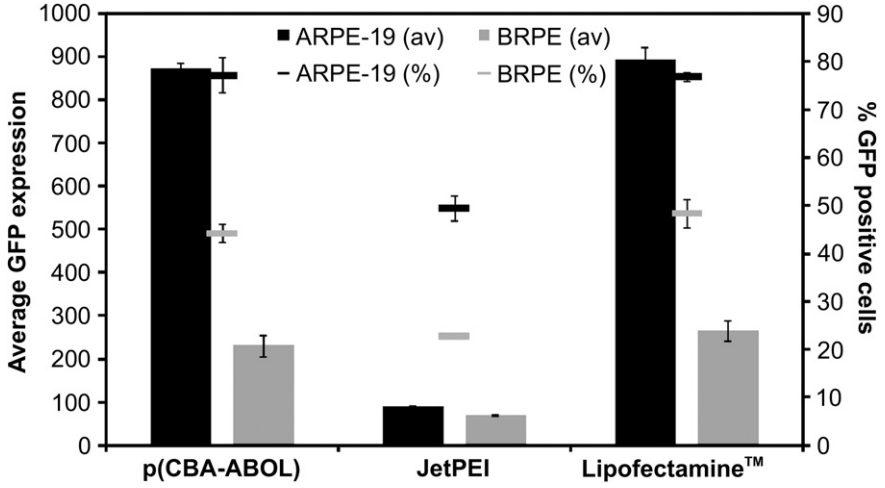

Fig. 1. Comparison of transfection efficacies between different gene carriers p(CBA-ABOL), JetPEI and Lipofectamin2000. Cells were transfected with a GFP reporter plasmid using three different carriers and subsequently washed with cell culture medium. Transfection levels were determined 24 h after transfection using flow cytometry showing the percentage of fluorescent cells (dots) and the average transgene GFP expression (bars). Transfection was assessed on both a continuous cell line (ARPE-19, in black) and primary bovine RPE cells (BRPE, in gray). Experiments were performed in triplicate and error bars represent standard deviations.

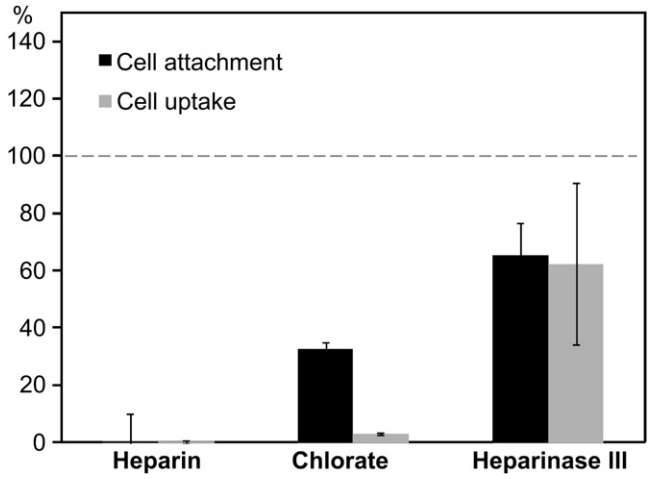

Fig. 2. Cellular attachment and uptake of p(CBA-ABOL)/DNA gene complexes is mediated by cell surface heparan sulfate proteoglycans. Cell attachment (black bars) and internalization (gray bars) of p(CBA-ABOL) polyplexes in ARPE-19 cells are shown. The remaining cell attachment or uptake is expressed as a relative percentage, normalized to untreated cells (represented by the dashed horizontal line). Experiments were performed in triplicate and error bars represent standard deviations.

fluid phase endocytosis [36]. We observed no inhibitory effect of sodium chlorate treatment on fluid phase endocytosis, nor on CDE (data not shown), demonstrating the specificity of this treatment. In contrast, desulfation of HSPGs reduces cell attachment of p(CBA-ABOL) polyplexes by more than 60% (Fig. 2) and consequently, cell uptake of the polyplexes is almost completely inhibited. Overall this indicates the necessity of sulfate groups on the cell surface for polyplex attachment and subsequent internalization.

Finally, as a third complementary strategy, the effect of heparan sulfate hydrolysis on polyplex attachment and endocytosis was examined through treatment with Heparinase III, a heparan sulfate lyase that exclusively cleaves heparan sulfate [37]. ARPE-19 cells were pretreated with this enzyme for 2 h in OptiMEM. p(CBA-ABOL) polyplexes were then added for 2 h in OptiMEM containing fresh Heparinase III. As shown in Fig. 2, this treatment significantly reduced polyplex attachment and to a comparable extent, polyplex uptake. However, in comparison to sodium chlorate treatment, the effect on polyplex internalization is less pronounced. The effect of Heparinase III treatment, however, confirms the particular involvement of heparan sulfate moieties of HSPGs for cell attachment of a significant fraction of p(CBA-ABOL) polyplexes in serum free conditions. Overall, we find that the electrostatic interaction between the cationic p(CBA-ABOL) polyplexes and the negatively charged HSPGs on the cell surface promotes efficient polyplex attachment and uptake.

3.3. *Unraveling the involvement of endocytic pathways: chemical inhibitors*

To unravel the involvement of known endocytic pathways in the internalization of p(CBA-ABOL) polyplexes, we inhibited endocytic processes using chemical inhibitors: chlorpromazine (Cpz), genistein, nocodazole, methyl-β-cyclodextrin (MβCD), cytochalasin D (CytoD), dynasore and rottlerin (Fig. 3). Drug induced cytotoxicity, the extent of inhibition and specificity of these endocytic inhibitors is cell-type-dependent [19] and we therefore first characterized the

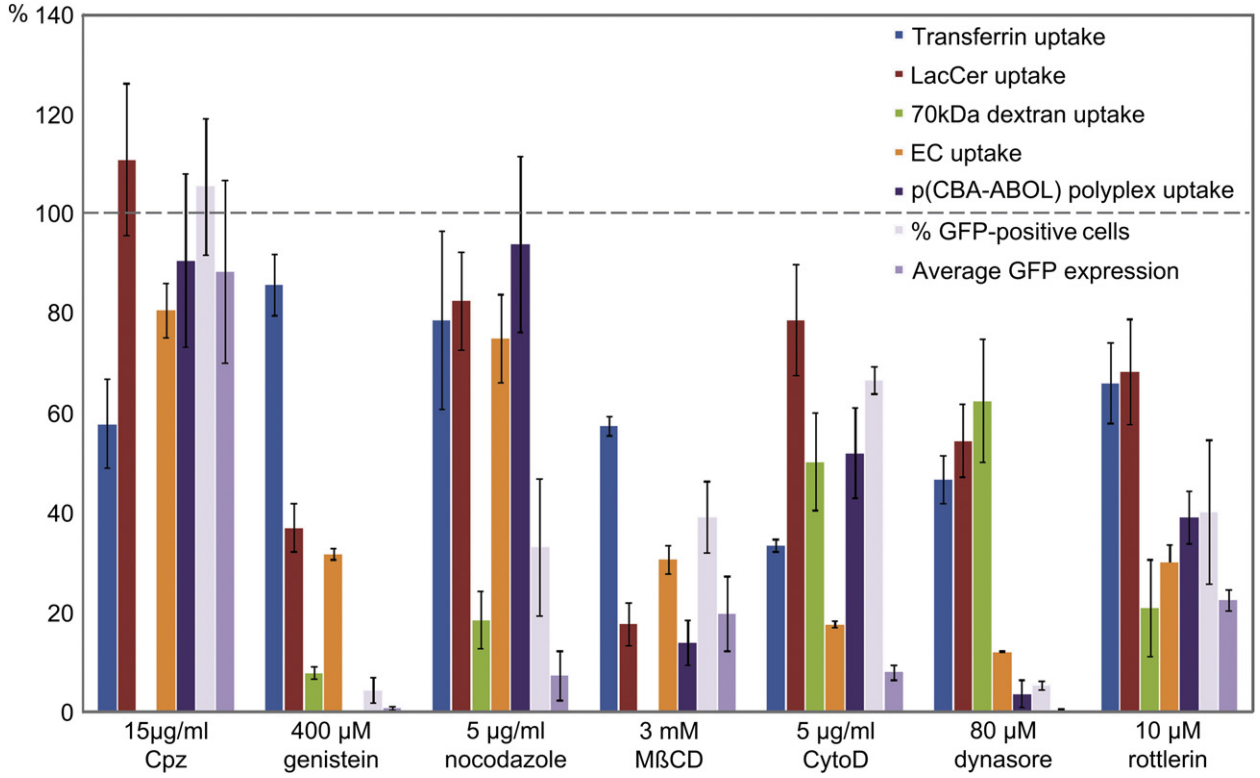

Fig. 3. Internalization of fluorescently labeled endocytic markers (transferrin, LacCer, 70 kDa dextran and ECs) and p(CBA-ABOL) polyplexes, and transfection efficiency following treatment with endocytic inhibitors in ARPE-19 cells. Measurements were performed by flow cytometry. The remaining cell uptake is expressed as a relative percentage, normalized to untreated cells (represented by the dashed horizontal line). Transfection of GFP reporter gene was quantified 24 h later as the average expression per cell and as the percentage of positively transfected cells, again both normalized to the fluorescence of untreated cells (dashed line). Experiments were performed in triplicate and error bars represent standard deviations. (Cpz: chlorpromazine; MβCD: methyl-β-cyclodextrin; CytoD: cytochalasin D).

effect of these inhibitors on several possible endocytic uptake routes in ARPE-19 cells using four fluorescently labeled endocytic markers: hTf, LacCer, dextran and ECs. Fluorescently labeled hTf is used as a marker for CDE. The glycosphingolipid LacCer resides preferably in lipid rafts and is reported to be internalized via Cav-ME [38] and is used here as a marker for CIE. Because of the lack of unique macropinocytic markers [39], fluid phase endocytosis of 70 kDa dextran molecules has often been measured as a marker for this process. Dextran uptake in unstimulated cells represents a combination of constitutive fluid phase endocytosis and possible constitutive macropinocytosis that is known to operate in some cell types. To qualitatively check ARPE-19 cells for constitutive macropinocytosis, they were incubated for 3 h with fluorescently labeled 70 kDa dextran. Supplementary. Fig. 5 demonstrates that a fraction of the cells contained intracellular μm-sized vacuoles, likely to be macropinosomes, resulting from constitutive macropinocytosis. This suggests that at least a part of the dextran is internalized via constitutive macropinocytosis. As a marker for phagocytosis, we used fluorescently labeled *E. coli* Bioparticles™ (ECs). The effects on the endocytic markers after inhibitor treatment in ARPE-19 cells is shown in Fig. 3 (Blue, red, green and orange bars), including the effect of the same inhibitors on polyplex uptake (dark purple bars). To correlate endocytosis route with gene delivery efficiency, we transfected cells with non-fluorescent polyplexes carrying the GFP reporter gene in the presence of endocytic inhibitors. Transfection efficiency is expressed both as percentage of fluorescent cells, and as average fluorescence level per cell (Fig. 3, two last light purple bars). Results from experiments with each type of inhibitor are discussed in turn below.

3.4. Depleting plasma membrane cholesterol

To assess the role of plasma membrane cholesterol, ARPE-19 cells were incubated with MβCD, a cyclic oligomer of glucopyranoside that inhibits cholesterol-dependent endocytic processes by reversibly extracting the steroid out of the plasma membrane [40]. MβCD is regularly used to determine whether endocytosis is dependent on the integrity of lipid rafts but has also been shown to inhibit CDE [40]. As can be seen from the results in Fig. 3, MβCD affected all endocytic markers as well as polyplex uptake and transfection. As can be expected, uptake of LacCer was reduced the most. However, all other endocytic markers were also affected by this treatment, which demonstrates the lack of specificity of this inhibitor for blocking subtypes of endocytic pathways. Despite this, the results indicate that the presence of cholesterol in the plasma membrane is indispensable for uptake of p(CBA-ABOL) polyplexes and their capacity for effective transfection.

3.5. Blocking actin and microtubule dynamics

CytoD is a fungal alkaloid that binds the barbed, fast growing plus ends of actin microfilaments and therefore blocks further polymerization and elongation of actin [41,42]. Actin disruption was visually confirmed on confocal microscopy images by staining the actin network in paraformaldehyde fixed cells with AF488 labeled phalloidin (results not shown). Data in Fig. 3 clearly show that actin polymerization is necessary for CDE, fluid phase endocytosis and phagocytosis; CIE is also affected, although to a lower extent. Interestingly, polyplex internalization is only partially (50%) dependent on actin polymerization, despite the substantial decrease of GFP expression. This suggests that actin polymerization is essential for successful intracellular processing of the internalized polyplexes.

Nocodazole induces depolymerization of the microtubules, which impairs the molecular motor-driven transport of vesicles on these tubular cytoskeletal structures [43]. Nocodazole treatment strongly inhibits the uptake of 70 kDa dextran but has only minor effects on the other endocytic probes including polyplexes (Fig. 3). This drug also had pronounced inhibitory effects on transfection efficiency. According to the proton sponge theory, endosomal acidification is necessary to enable polyplexes, composed of polymers with high buffer capacities around physiological pH, to escape from the endosomes into the cytoplasm and to cause successful gene transfer [44]. It is known that microtubule integrity is necessary for maturation of early/sorting endosomes to late endosomes with the accompanying drop in luminal pH [45,46]. These results suggest that nocodazole probably inhibits endosomal escape of the polyplexes by inhibiting the luminal acidification of the endosomes.

Overall, these results suggest that p(CBA-ABOL) polyplexes are internalized in ARPE-19 cells via an endocytic mechanism that relies on local actin polymerization but not on microtubule integrity.

3.6. Role of CDE

To investigate the involvement of CDE, we applied Cpz, a cationic amphiphilic drug which is believed to inhibit clathrin-coated pit formation by a reversible translocation of clathrin and its adapter proteins from the plasma membrane to intracellular vesicles [47]. As expected, Cpz treatment inhibits hTf uptake, an established CDE marker (See Fig. 3). In contrast, it does not inhibit LacCer uptake, nor polyplex uptake or transfection. This indicates that CDE does not play a significant role in polyplex uptake. This conclusion is corroborated by the genistein data (See Fig. 3). Genistein, a well-characterized inhibitor of tyrosine kinase mediated signal transduction [48], has only a slight effect on CDE, while clearly inhibiting fluid phase uptake, phagocytosis, CIE and completely blocking polyplex uptake. From the Cpz and genistein data we conclude that polyplex uptake is primarily independent of CDE.

3.7. Blocking dynamin function with dynasore

Because dynamin is a regulatory protein for several endocytic pathways, we assessed its role in cell uptake of the polyplexes. This large GTPase forms a helical polymer around the neck of a newly invaginated endosome and catalyzes upon GTP hydrolysis the fission of the vesicle from the plasma membrane. Dynamin has been shown to regulate CDE, Cav-ME and phagocytosis [49]. To assess the role of dynamin in polyplex uptake, ARPE-19 cells were incubated with dynasore, an inhibitor of the GTPase activity of both dynamin-1 and 2 isoforms [50]. Dynasore, as predicted, inhibited EC uptake and 50% of hTf uptake (Fig. 3) and reduced, though to a lower extent, uptake of both 70 kDa dextran and LacCer. Dynasore treated cells were unable to internalize polyplexes, indicating that dynamin function is essential for p(CBA-ABOL) polyplex endocytosis in ARPE-19 cells.

3.8. Inhibition of PKC signaling

To investigate the role of macropinocytosis, we treated the cells with rottlerin, a polycyclic aromatic compound inhibiting protein kinases C (PKC) [51] and reported to be a fairly selective inhibitor of constitutive macropinocytosis [52]. Fig. 3 demonstrates that rottlerin slightly inhibited the uptake of hTf and LacCer and exhibited a pronounced inhibition of polyplexes, ECs and fluid phase uptake of 70 kDa dextran molecules. Since rottlerin seems to affect both fluid phase endocytosis and phagocytosis, it does not provide further information on the possible specific involvement of macropinocytosis on polyplex internalization.

However, the response of the polyplexes and dextran to inhibitors like dynasore and nocodazole was very different. In particular, after nocodazole treatment, complete inhibition of 70 kDa dextran uptake was observed, while uptake of the complexes was similar to untreated cells (Fig. 3). In case of dynasore, polyplex uptake was completely inhibited, while 70 kDa dextran uptake was reduced by only 40%. This would suggest that fluid phase uptake and constitutive macropinocytosis is not correlating with p(CBA-ABOL) polyplex uptake in ARPE-19 cells. In contrast, the results in Fig. 3 generally show a strong correlation between EC and polyplex endocytosis in response to these pharmacological inhibitors. This suggests phagocytosis as a potential uptake route for p(CBA-ABOL) polyplexes in ARPE-19 cells.

3.9. Unraveling the involvement of endocytic pathways: RNAi

To complement the chemical inhibitor studies, RNAi was implemented in this work to downregulate expression of key endocytic proteins thus inhibiting specific endocytic pathways. The targeted proteins were clathrin heavy chain (CHC), caveolin-1 (Cav1), flotillin-1 (Flot1), GTPase regulator associated with focal adhesion kinase (GRAF1), ADP ribosylation factor 6 (Arf6), dynamin-2 (DNM2) and serine/threonine-protein kinase (PAK1). A list of the corresponding siRNA sequences, used in this work, is given in Supplementary. Table. 1. Downregulation was assessed by Western blotting (Fig. 5). The same flow cytometry methods were used to evaluate the effects on endocytic uptake and transfection of the GFP reporter gene (Fig. 4).

3.10. Role of heavy chain clathrin

As expected, depleting the expression of clathrin heavy chain inhibited transferrin uptake by 80% (Fig. 4), however we were surprised to observe that the same depletion caused an induction in the uptake of all other endocytic markers, including polyplexes. In any case, this confirms that internalization of p(CBA-ABOL) polyplexes in ARPE-19 cells is independent of CDE. The depletion in expression of CHC was clearly confirmed by Western blotting (Fig. 5A).

3.11. Role of DNM2 function

To confirm the involvement of dynamin in polyplex uptake, we downregulated DNM2 expression with the help of RNAi [53] and Western blotting demonstrated at least a partial reduction in protein expression (Fig. 5B). In agreement with the dynasore data, DNM2 downregulation significantly inhibited hTf, EC and polyplex uptake (Fig. 4), although LacCer and 70 kda dextran uptake was not inhibited, despite the significant inhibitory effect of dynasore. Indeed, it was previously reported that selective knockdown of DNM2 may still permit CIE of cholera toxin subunit B (CtxB) and fluid phase endocytosis, possibly because DNM1 adopts the role of DNM2 for vesicle fission [54]. Finally, Fig. 4 also shows that DNM2 depletion results in substantial reduction of transgene expression, indicating that the endocytic pathways that lead to successful transfection are dynamin dependent.

3.12. Role of Cav1 and Flot1

Combined, the experiments with chemical endocytic inhibitors suggested that CDE is not involved in polyplex uptake. However, the inhibitors did not allow us to distinguish between different subclasses of CIE pathways. To evaluate the specific involvement of Cav-ME and Flot-ME, two known subclasses of CIE, we used RNAi to downregulate the expression respectively of Cav1 and Flot1. Depletion of these two proteins was again confirmed by Western blotting (Fig. 5C). As shown in Fig. 4, Cav1 downregulation, as predicted, inhibited a fraction of LacCer uptake, but there was no

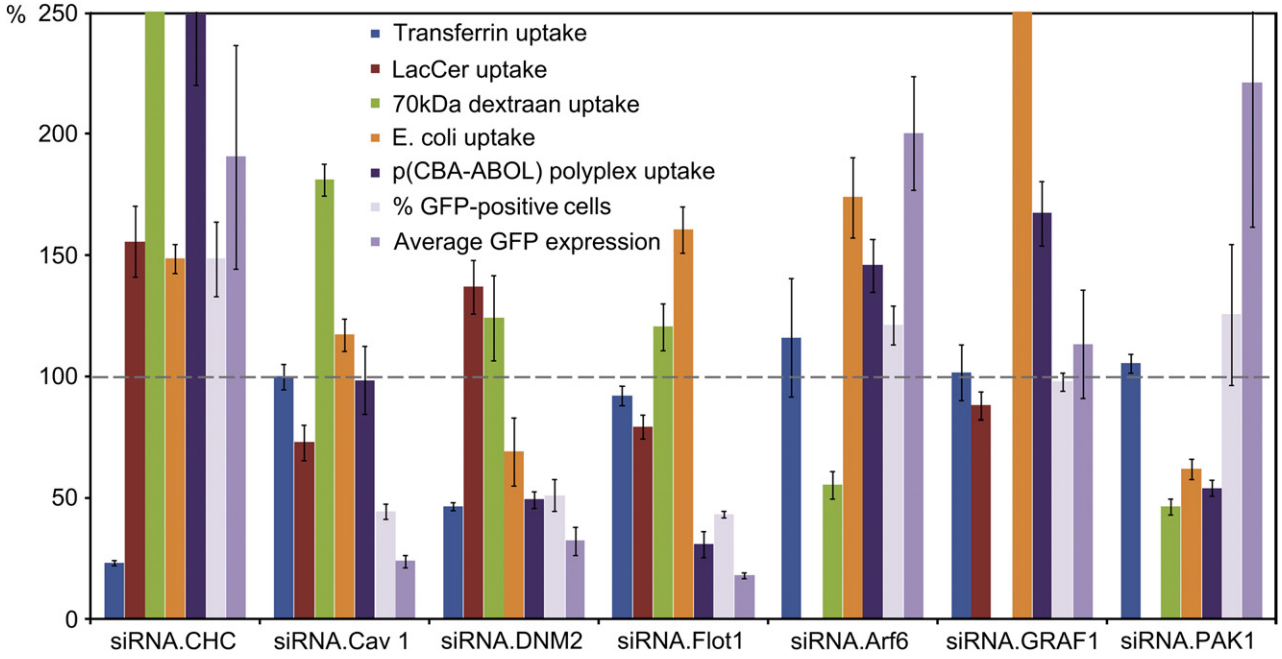

Fig. 4. Internalization of fluorescently labeled endocytic markers (transferrin, LacCer, HMW dextran and ECs), p(CBA-ABOL) polyplexes, and transfection efficiency after siRNA mediated depletion of endocytic proteins in ARPE-19 cells. Measurements were performed by flow cytometry. The remaining cell uptake is expressed as a relative percentage, normalized to cells, treated with NC siRNA (represented by the dashed horizontal line). Transfection of the GFP reporter gene was measured again 24 h later and was both quantified as the average expression per cell and as the percentage of positively transfected cells, again both normalized to the cell population, transfected with negative control siRNA. Experiments were performed in triplicate and error bars represent standard deviations. (CHC: clathrin heavy chain; Cav1: caveolin-1; Flot1: flotillin-1; GRAF1: GTPase Regulator Associated with Focal Adhesion Kinase; Arf6: ADP ribosylation factor 6; DNM2: dynamin-2; PAK1: Serine/threonine-protein kinase).

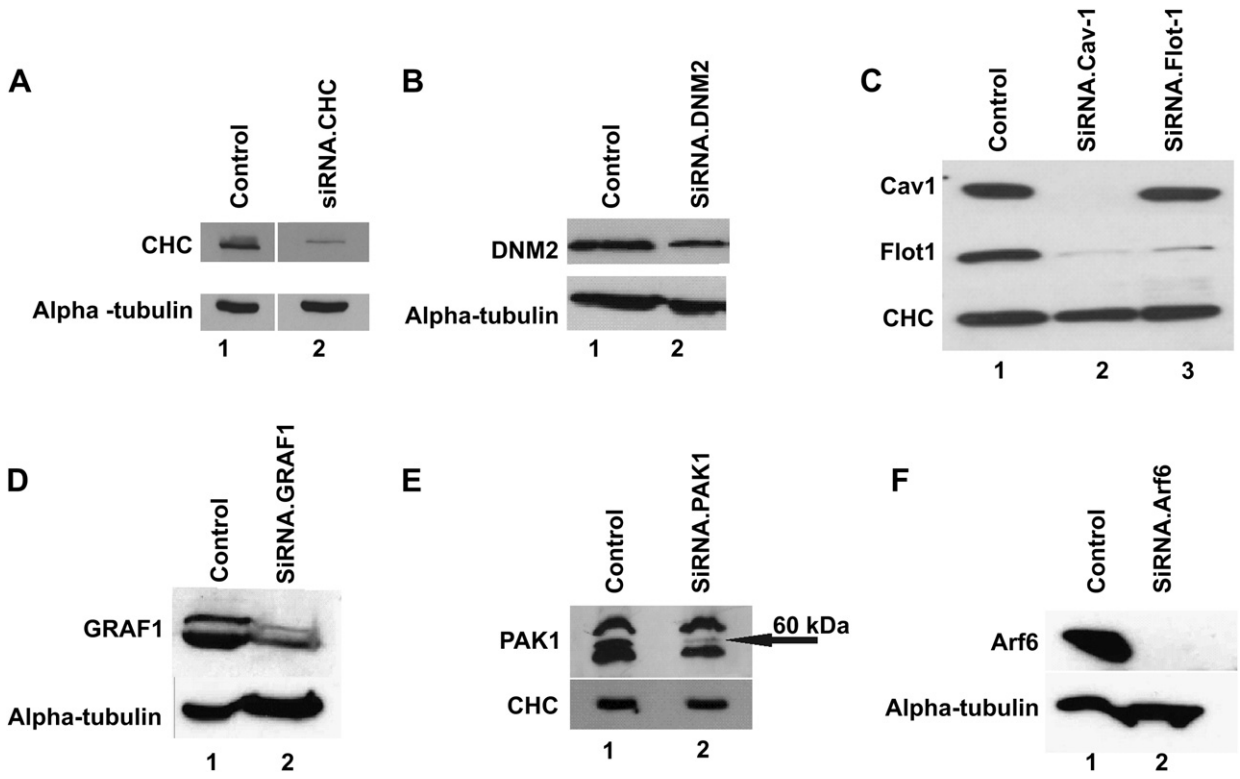

Fig. 5. Protein expression after siRNA downregulation, visualized by Western blotting. In all cases, the control cells were treated with negative control siRNA (Supplementary. Table. 1). For (A), (B), (D) and (F) the expression of α-Tubulin served as an internal control for equal protein loading, while CHC expression levels were used as a reference in (C) and (E). In (E), the PAK1 band of 60 kDa is marked with a black arrow. (CHC: clathrin heavy chain; Cav1: caveolin-1; Flot1: flotillin-1; GRAF1: GTPase regulator associated with focal adhesion kinase; Arf6: ADP ribosylation factor 6; DNM2: dynamin-2; PAK1: Serine/threonine-protein kinase).

effect on uptake of any of the other endocytic markers or polyplexes. Interestingly, transfection was clearly less successful in the absence of Cav1, suggesting a crucial role for this protein in gene transfer with p(CBA-ABOL) polyplexes. The observed role of Cav1 in gene transfer may here be indirect, and not related to endocytosis, noting that Cav1 knockdown appears not to inhibit polyplex endocytosis. Conversely, Flot1 downregulation inhibited both polyplex uptake and transfection. We therefore conclude that Flot-ME is not only involved in p(CBA-ABOL) polyplex endocytosis in ARPE-19 cells, but also contributes to successful transfection. This demonstrates the importance of Flot-ME as a portal to the cell for successful gene transfer.

3.13. Role of the CLIC/GEEC pathway

A recently defined CIE pathway, independent of Cav1 and Flot1, is the CLIC/GEEC pathway. This portal plays a major role in the endocytosis of certain GPI linked proteins [55]. The cargoes are collected in tubular invaginations, called clathrin-independent carriers (CLIC's), and are trafficked to Rab5-independent endosomes, called GPI-enriched endosomal compartments (GEEC's). Other cargoes like Cholera toxin subunit B (CtxB), Simian Virus 40 (SV40) and Shiga toxin were also found to be internalized via this pathway [53]. This pathway is also reported to be responsible for a major fraction of fluid phase uptake and is independent of DNM2 [56]. We therefore investigated its role in entry of the endocytic markers and polyplexes by depleting GRAF1, a protein shown to regulate this pathway [57]. Efficient GRAF1 depletion was confirmed by Western blotting (Fig. 5D). Downregulation of GRAF1 didn't decrease polyplex internalization (Fig. 4), suggesting a lack of involvement of the CLIC/GEEC pathway. Interestingly, we observed that GRAF1 knockdown stimulated both polyplex and phagocytosis uptake, but not transgene GFP expression.

3.14. Role of PAK1 and Arf6

To further elucidate the possible involvement of macropinocytosis, we depleted expression of PAK1 and Arf6, two proteins that have been shown to regulate this process [39,58]. PAK1 is a serine/threonine kinase, regulating cytoskeleton dynamics and motility; upon activation, it relocates to the plasma membrane where it activates a variety of effectors, such as BARS, needed for ruffling, blebbing and macropinosome formation [59]. Knockdown of PAK1 kinase expression in ARPE-19 cells was successful according to Western blot analysis (Fig. 5E). Two other bands were also observed with the anti-PAK1 antibody but their expression was insensitive to PAK1-siRNA. Fig. 4 shows that PAK1 downregulation had no effect on hTf internalization, while cell uptake of polyplexes and fluid phase marker 70 kDa dextran were reduced by 50%. Surprisingly, PAK1 downregulation also decreased EC uptake, suggesting an additional role for this protein in ARPE-19 phagocytosis. Despite PAK1 having a significant role in polyplex endocytosis, transfection was not inhibited (Fig. 4). We conclude that, while either macropinocytosis or phagocytosis contributes to endocytosis of our polyplexes, this PAK1- dependent pathway does not contribute to successful gene transfer.

Arf6 is a member of the Arf family of small GTPases, which are involved in the regulation of membrane structure and transport [60], and is known to be a positive modulator of MP [39]. Successful knockdown of this protein (Fig. 5F) led to a decrease in 70 kDa dextran uptake, while endocytosis of both ECs and p(CBA-ABOL) gene complexes was induced (Fig. 4). This suggests that constitutive

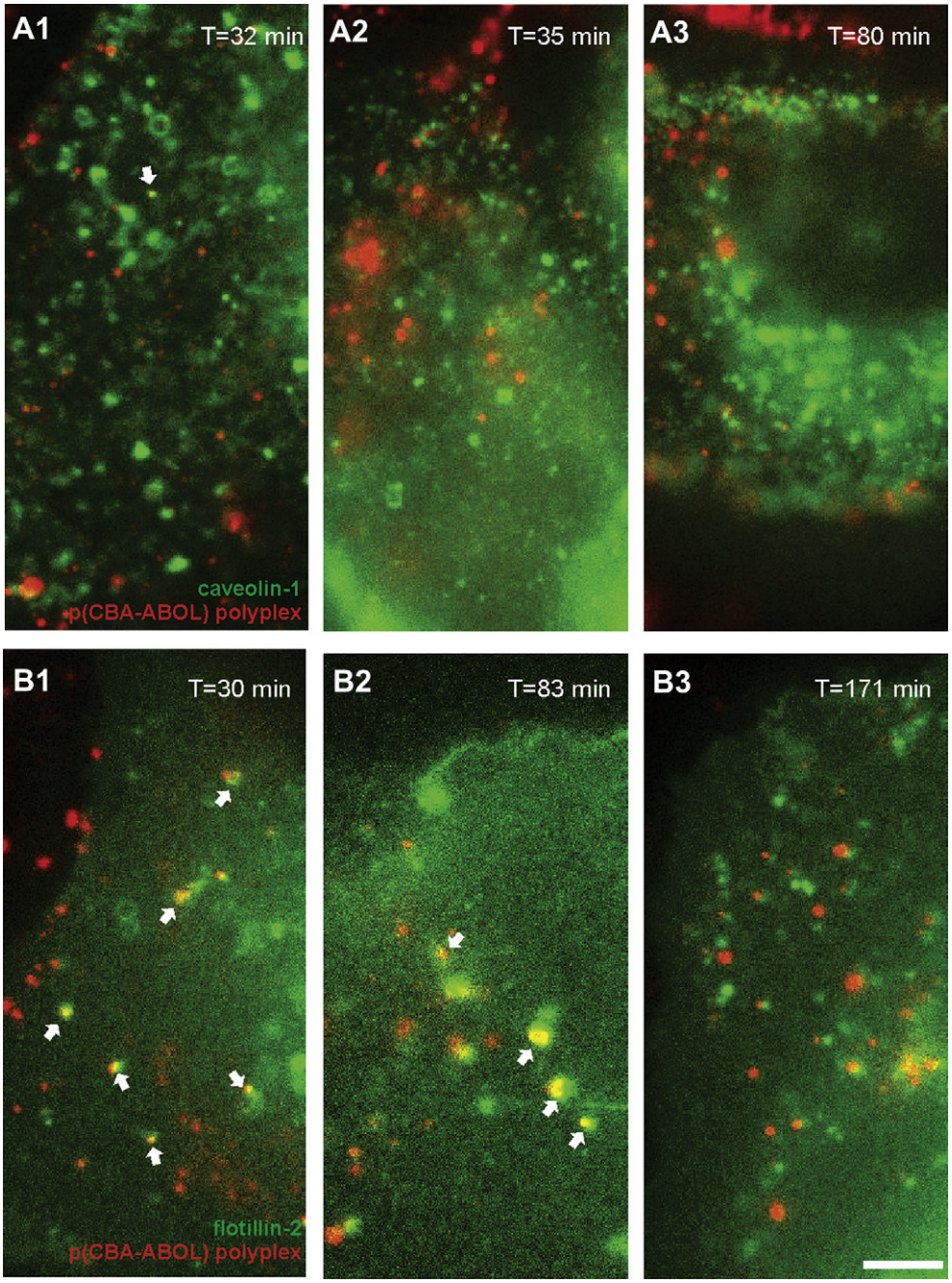

Fig. 6. Colocalization of p(CBA-ABOL) polyplexes with flotillin or caveolin containing vesicles in living ARPE-19 cells. Cells transfected with (A) Cav1-EGFP and (B) Flot2-EGFP were exposed to p(CBA-ABOL) Cy5-pDNA polyplexes for 15 min. After washing, the cells were transferred in a stage top incubator and imaged on a wide field fluorescence microscope in OptiMEM. Fluorescence images, selected from livecell time-lapse movies show colocalization of the polyplexes at early timepoints with Flot2 (B1 and 2), which disappears at later timepoints (B3). The white arrows show colocalizing signals. Very little colocalization is observed between the Cy5-labeled plasmids and Cav1, either at early (A1) or at later timepoints (A2 and 3). Scale bar is 5 μm.

macropinocytosis is not involved in the internalization of p(CBA-ABOL) polyplexes.

3.15. Live cell fluorescence colocalization microscopy

Aside from inhibiting endocytic pathways with chemical inhibitors and siRNA depletion, fluorescence microscopy was utilized to probe further the involvement of Cav-ME or Flot-ME in the initial uptake of p(CBA-ABOL) polyplexes. Cells were transfected with plasmids encoding EGFP-Flot2 or EGFP-Cav1 for visualization of flotillin or caveolin containing endosomes, respectively. It is believed that coassembly of both Flot1 and Flot2 is necessary for Flot-ME to occur [61]. Caveolin containing endosomes are typically termed cavicles and caveosomes [7]. GFP fusion proteins were clearly expressed after 24 h and they were then incubated with p(CBA-ABOL) polyplexes containing Cy5-labeled plasmids. After 15 min of incubation with the polyplexes, cells were washed with OptiMEM and observed as live cells on a stage top incubator by fluorescence microscopy. We clearly observed colocalization within 30 min between polyplexes and flotillin-2 (Fig. 6B1 and 2), which generally disappeared about 150 min after initial incubation with polyplexes (Fig. 6B3). In contrast, virtually no colocalization was

observed between polyplexes and caveolin-1 (Fig. 6A1-3). These observations provide further evidence that p(CBA-ABOL) polyplexes are internalized in flotillin-vesicles rather than caveosomes.

4. Discussion

The RPE is an attractive target for treating diseases such as AMD or retinitis pigmentosa with non-viral nucleic acid carriers following subretinal or intravitreal injection. However the efficiency of subcellular delivery of therapeutic nucleic acids into these cells remains low. The carrier defines the mechanisms that direct cell attachment, subsequent endocytosis and intracellular trafficking and therefore strongly determines transfection efficiency. A better understanding of these mechanisms will help to improve the design of efficient CBA based polymeric carriers since little information is currently available on cellular adhesion, intracellular uptake and intracellular processing of p(CBA-ABOL) polyplexes in RPE cells. Here, we studied cell attachment and endocytosis of polyplexes, composed of the novel bioreducible polymer p(CBA-ABOL) and plasmid DNA. We first focused on cell attachment and proceeded with characterizing the endocytic pathways that are involved in their subsequent uptake by using a combination of pharmacological inhibitors, RNAi knockdown and live cell fluorescence colocalization microscopy.

4.1. In vitro evaluation of p(CBA-ABOL) as a carrier for gene delivery in RPE cells

First, we compared the *in vitro* transfection potential of different carriers on both a continuous RPE cell line and primary bovine cells (BRPE). Overall, the data showed p(CBA-ABOL) to be a promising transfection agent in both cultured and primary cells, outperforming linear PEI and equaling commercial liposome based systems. JetPEI polyplexes transfected only 50% of the cells, which we believe is a consequence of significantly lower cell uptake (4–5 times) during the 2 h exposure time, when compared with the other carrier systems (See Supplementary. Fig. 6). In primary cells, transfection efficiency was lower for all carriers and this is probably due to general lower internalization rates, because we observed that only about half of the amount of p(CBA-ABOL) and Lipofectamin2000™ complexes are internalized in BRPEs cells compared to the RPE cell line (ARPE-19) (See Supplementary. Fig. 6). This is possibly due to their lower metabolic, and therefore lower endocytic activity. In line with this, we observed significant lower cellular growth rates for the primary RPE cells.

4.2. Role of anionic cell surface proteoglycans in p(CBA-ABOL) polyplex attachment and internalization

We identified that the interaction between cationic polyplexes and cell surface HSPGs is essential for efficient internalization. This is in agreement with reports for other types of cationic complexes and can be easily explained by the electrostatic interaction between the positively charged gene carrier and negatively charged heparan sulfate chains [14,34,62,63]. In order to ascertain the rate of polyplex internalization and identify optimal incubation times for cells with the polyplexes, we also evaluated their uptake kinetics in ARPE-19 cells (Supplementary. Fig. 3). Similar to what was found for other gene delivery vehicles, viral and non-viral [1,15], we observed that p(CBA-ABOL) polyplexes are rapidly taken up in ARPE-19 cells and that this internalization is saturated after 2 h. The internalization kinetics follow a sigmoid-like function which is typical for an endocytic uptake pattern because of saturation of the endocytic machinery. These results suggest that general cellular uptake as such is not the bottle neck for efficient transfection, at least in the absence of anionic biopolymers.

4.3. p(CBA-ABOL) polyplex uptake via a PAK1 dependent phagocytosis-like mechanism

As a first strategy to identify the endocytic pathway(s) utilized by p(CBA-ABOL) complexes to enter ARPE-19 cells, we made use of chemical endocytic inhibitors. We have recently shown that chemical endocytic inhibitors should be used with care as their effect is highly cell-type-dependent and not as specific as they are often reported to be [19]. Therefore, alongside our polyplexes, we evaluated the effect of these inhibitors on several types of endocytic markers. These results suggested that polyplex uptake does not involve CDE but is strongly dependent on cholesterol, tyrosine kinase activity and dynamin as well as on actin and PKC activity. Several reports link HSPG mediated endocytosis to macropinocytosis [32,64,65], also in cellular uptake of cationic gene delivery vehicles [15,65–67]. However, Kopatz et al. discovered close similarities between HSPG-dependent phagocytosis in epithelial cells and endocytosis of PEI/DNA polyplexes [62]. Moreover, it has previously been suggested that viruses like HSV-1 can infect both professional and non-professional phagocytes via a phagocytosis-like mechanism after heparan sulfate binding [68]. Despite the difficulties of distinguishing between the involvement of macropinocytosis and phagocytosis in nanomedicine uptake, since there are no chemical inhibitors that are specific for either of them, we were able to come to some conclusions on this matter based on several observations. First, using nocodazole and dynasore, we found marked opposite inhibitory effects for uptake of polyplexes and 70 kDa dextran, the latter often being used as a marker for constitutive macropinocytosis. Interestingly, we found a strong correlation between cellular internalization of the polyplexes and *E. coli* particles, the latter being an established marker for phagocytosis. Second, while actin, tyrosine kinases and PKC, all appear to be required for polyplex uptake in ARPE-19 cells and are known criteria for macropinocytosis [39], these proteins also regulate phagocytosis (Fig. 3) [39] and therefore do not exclude the involvement of a phagocytosis-like mechanism. Third, dynamin is often known to play a redundant role in macropinocytosis [69], though its function is essential for phagocytic cup closure [39]. Using dynasore to block all dynamin isoforms, this study showed a noticeable dependence on dynamin function during polyplex endocytosis, which is again in favor of the involvement of a phagocytosis-like mechanism.

As a second strategy to identify the involvement of endocytic pathway(s) during polyplex endocytosis, we depleted key endocytic proteins with the help of RNAi. By depleting DNM2, we could confirm the involvement of this protein for polyplex uptake. Furthermore, when depleting PAK1 and Arf6 which are both reported to regulate macropinocytosis [39], we observed that Arf6 did not have any inhibitory effect on polyplex uptake, providing further evidence that macropinocytosis is probably not involved in p(CBA-ABOL) polyplex endocytosis. The involvement of PAK1 during polyplex endocytosis could then be attributed to its involvement in phagocytosis in ARPE-19 cells. Indeed, it has been previously reported that PAK1 plays a role in actin rearrangements during phagocytosis [70,71]. The effect of PAK1 knockdown on polyplex uptake could therefore be assigned to the inhibition of phagocytic uptake of the polyplexes.

Finally, it should be noted that our polyplexes have the tendency in physiologic media of high ionic strength to form spherical aggregates with sizes up to 5 μm (Supplementary. Fig. 7). Therefore, the cells were exposed to polyplexes with a wide distribution of sizes. Since the RPE is *in vivo* the most active phagocytic tissue in humans [21], it is unsurprising that these large aggregates were

observed to be internalized in ARPE-19 cells. Taken together, despite the inability to specifically inhibit phagocytosis, our observations suggest that a PAK1 dependent, phagocytosis-like mechanism is involved in the cellular internalization of p(CBA-ABOL) polyplexes in ARPE-19 cells.

4.4. p(CBA-ABOL) polyplex uptake via flotillin-dependent endocytosis

Despite excluding a role for CDE in polyplex uptake, the chemical inhibitors could not differentiate between the various CIE routes. CIE like Cav-ME is often reported to be involved in internalization of non-viral gene delivery vehicles [13]. To discriminate between different CIE pathways, we employed siRNA depletion studies and found no involvement of Cav-ME, the CLIC/GEEC pathway, nor Arf6-dependent endocytosis for polyplex uptake. However, p(CBA-ABOL) polyplex internalization was found to be dependent on DNM2, Flot1 and PAK1. As discussed above, the involvement of PAK1 can be related to phagocytic uptake. Interestingly, however, the strong dependency on Flot1 suggests Flot-ME as an important alternative entry route. To verify this, we investigated the colocalization of flotillin-2 positive vesicles and the polyplexes using livecell dual color fluorescence microscopy. Polyplexes resided within flotillin-2 positive vesicles within 30 min after transfection, but there was no evidence of their association with caveolin and thus caveolae. This is in agreement with a recent study on the uptake of PEI polyplexes and Lipofectamine™ lipoplexes in HeLa cells [14], where a link was found between the attachment of gene complexes to cell surface HSPGs and subsequent Flot-ME of HSPG bound gene complexes. Knowledge of HSPG endocytosis is still quite limited, despite its essential role in the internalization of some viruses, bacteria and cationic peptides [31]. After interacting with heparan sulfate binding ligands, HSPGs are reported to cluster in cholesterol-dependent micro-environments that are internalized in endocytic vesicles deficient of caveolin-1 and clathrin, but positive for flotillin-1. This process requires an intact actin cytoskeleton tyrosine kinase activity, PKC activity, dynamin and activated Rac [72]. This is in strong agreement with our findings here. Whether DNM2 is required for Flot-ME seems to depend on the nature of the internalized cargo. For example, DNM2 is not required for HSPG mediated internalization of eosinophil cationic protein in Beas-2B cells [64], but was shown to be required for HSPG mediated uptake of PEI polyplexes in HeLa cells [14]. This is in good agreement with our findings for p(CBA-ABOL) polyplexes in RPE cells. We conclude that, apart from phagocytosis, the p(CBA-ABOL) polyplexes enter ARPE-19 cells through Flot-ME.

It is accepted that nanoparticle size can have a substantial influence on endocytic uptake of nanomedicines [73], which is attractive in the sense that it would offer possibilities to target for preferred endocytic pathways simply by engineering the size of the nanomedicines. In this study we have found that the p(CBA-ABOL) polyplexes aggregate when suspended in OptiMEM. This could be easily demonstrated using fluorescence single particle tracking (see Supplementary. Fig. 7) [74]. In an attempt to study the influence of size on uptake, we have performed extra experiments in which the polyplexes were first incubated for 30 min in OptiMEM before adding them to the cells. This will increase the extent of aggregation and could give some preliminary insight if the identified endocytosis pathways depend on the size of the complexes. As summarized in Supplementary. Fig. 8, while the polyplex uptake and transfection was increased when pre-incubated in OptiMEM, we could not find a shift in endocytosis pathways, at least as far as the PAK1 and flotillin-1-dependent or Flot-1-dependent routes are concerned. Although this is not a stringent proof, it is a first indication that the results published here, perhaps surprisingly, are not size dependent.

4.5. Correlation between endocytosis and transgene expression

Having established that p(CBA-ABOL) polyplexes are internalized in ARPE-19 cells via a phagocytosis-like mechanism and Flot-ME, it remained to be determined whether they are equally involved in mediating transfection. It is important to evaluate whether certain endocytic pathways preferentially lead to cell transfection, as it would allow one to consider a strategy to target the polyplexes towards the most successful endocytic pathway through ligand coupling. Using siRNA depletion of flotillin-1 we could clearly show that Flot-ME is an important route for transfection. In contrast, despite the significant role of PAK1 in polyplex uptake, PAK1 knockdown did not decrease GFP expression. This suggests that the phagocytosis-like internalization of polyplexes is not as effective for transfection and this could be due to the instant delivery of the polyplexes through phagosomes to degradative lysosomes.

In addition, we observed an intriguingly strong effect of caveolin-1 depletion on reporter gene expression, despite the fact that polyplex uptake was relatively unaffected. Since this protein was not shown to play a major role in early intracellular trafficking of p(CBA-ABOL) polyplexes (Fig. 6), this suggests an indirect effect of Cav1 knockdown. Indeed, Fig. 5C clearly shows that knockdown of caveolin-1 resulted in a comparable downregulation of flotillin-1 expression. Interestingly, a similar though opposite effect has been reported in HeLa cells [75] and in intestinal epithelial cells [76]. To explain the observed effects on uptake and transfection, we propose the following hypothesis. Downregulating caveolin-1 results in a decrease of Flot-ME and thereby decreases polyplex uptake. At the same time caveolin-1 knockdown causes stimulation of phagocytosis (Fig. 4), resulting in a net unaltered uptake of polyplexes. However, because the induced phagocytosis-like internalization pathway of the polyplexes does not contribute to transfection, its overall efficiency drops.

4.6. Inhibiting endocytic pathways: chemical versus molecular inhibition

Chemical inhibitors are frequently used to study endocytosis and results generated from studies using these agents are often insightful. However, without adequate controls their effects are difficult to interpret and could give rise to erroneous conclusions. The experiments with genistein and resulting data highlight this issue. Genistein is frequently used to study Cav-ME functioning as a tyrosine kinase inhibitor that impairs actin recruitment and DNM2 recruitment to the site of endocytosis [48]; both are indispensable for Cav-ME. However, genistein treatment might also affect other endocytosis routes as we observed here and in fact our studies showed that CDE was the only endocytic pathway tested that was insensitive to this drug. Phagocytosis has been also shown to be sensitive for genistein [77,78] and Flot-ME is reported to be tyrosine kinase dependent [79]. Therefore, if genistein inhibits uptake of gene complexes, one cannot necessarily draw the conclusion that they are taken up by Cav-ME. Indeed, while we found that the uptake of p(CBA-ABOL) complexes is inhibited by genistein, RNAi depletion revealed that it is not Cav-ME but rather a combination of phagocytosis and Flot-ME that regulate polyplex uptake. Similar issues and difficulties in interpretation were encountered with rottlerin, a PKC inhibitor reported to inhibit macropinocytosis [52]. Macropinocytosis and phagocytosis have been reported to be PKC dependent [52], thus questioning the specificity of this drug. Indeed, our own results showed rottlerin to inhibit uptake of 70 kDa dextran, but it also inhibited 40% of EC uptake and 30% of hTf and LacCer uptake (Fig. 3).

It is clear that chemical inhibitors by itself are generally not sufficient to fully elucidate endocytosis of gene complexes or

nanoparticles in general. As demonstrated in this work, RNAi downregulation of specific proteins can provide further complementary data. It is however, important to note that not all cells will be evenly affected by siRNA and thus the cell population may be heterogeneous with respect to their level of expression of the target protein. To analyze the cells which were successfully depleted, cotransfection experiments with reporter gene forming a selection marker for knockdown cells are often employed [14]. Alternatively, to increase the probability of downregulating a majority of cells, one can repeatedly transfect the cells with siRNA [14,80]. It is the latter strategy that was applied in this work. Furthermore, siRNA mediated knockdown exhibits generally high specificity. However, in some cases protein downregulation can affect, directly or indirectly, expression of other proteins. These effects were also observed in our studies, where the siRNAs against caveolin-1 seemed to knockdown flotillin-1 expression (Fig. 5C).

5. Conclusion

In this work we performed a detailed study on the attachment and internalization mechanisms of p(CBA-ABOL) gene complexes in a *in vitro* model of the retinal pigment epithelium. To elucidate endocytic mechanisms, we encourage the combination of different methodological approaches, like chemical and RNAi based inhibition, which can be further complemented with dual color fluorescence colocalization microscopy. Here, we show that the polyplexes are internalized via two endocytic portals to the cell, after association with cell surface HSPGs. These portals are flotillin mediated endocytosis and a PAK1 dependent, phagocytosis-like mechanism. Interestingly we found that of both internalization routes, only Flot-ME leads to successful transfection. An elaborate comprehension of both the characteristics of the vectors as well as the mechanisms by which they interact with the targeted cells is required to eventually help us design safe and efficient non-viral gene vectors to transfect the RPE and, by extension, any other type of target cells. This knowledge may help us (1) to evaluate the effects of chemical modifications of the carrier polymer on cell attachment and endocytosis, (2) to identify new specific cell surface targets to improve cell attachment and (3) to aim for specific endocytic pathways that lead to successful transfection.

Acknowledgments

D. Vercauteren is a doctoral fellow of the Institute for the Promotion of Innovation through Science and Technology in Flanders (IWT), Belgium. We gratefully acknowledge the European Commission for funding through the Integrated 6th Framework Programme MediTrans. Monerah al Soraj is supported by a Kuwaity Government sponsored PhD studentship awarded to Cardiff University.

Appendix. Supplementary material

Supplementary data related to this article can be found online at doi:10.1016/j.biomaterials.2010.12.045.

References

[1] Varga CM, Tedford NC, Thomas M, Klibanov AM, Griffith LG, Lauffenburger DA. Quantitative comparison of polyethylenimine formulations and adenoviral vectors in terms of intracellular gene delivery processes. Gene Ther 2005;12:1023–32.
[2] Doherty GJ, McMahon HT. Mechanisms of endocytosis. Annu Rev Biochem 2009;78:31.1–31.46.
[3] Jones AT. Macropinocytosis: searching for an endocytic identity and role in the uptake of cell penetrating peptides. J Cell Mol Med 2007;11:670–84.
[4] Kerr MC, Teasdale RD. Defining macropinocytosis and others. Traffic 2009;10:364–71.
[5] Maxfield FR, Mcgraw TE. Endocytic recycling. Nat Rev Mol Cell Biol 2004;5:121–32.
[6] Mayor S, Pagano RE. Pathways of clathrin-independent endocytosis. Nat Rev Mol Cell Biol 2007;8:603–12.
[7] Pelkmans L, Helenius A. Endocytosis via caveolae. Traffic 2002;3:311–20.
[8] Glebov OO, Bright NA, Nichols BJ. Flotillin-1 defines a clathrin-independent endocytic pathway in mammalian cells. Nat Cell Biol 2006;8:46-U16.
[9] Doherty GJ, Lundmark R. GRAF1-dependent endocytosis. Biochem Soc Trans 2009;37:1061–5.
[10] Douglas KL. Toward development of artificial viruses for gene therapy: a comparative evaluation of viral and non-viral transfection. Biotechnol Prog 2008;24:871–83.
[11] von Gersdorff K, Sanders NN, Vandenbroucke R, De Smedt SC, Wagner E, Ogris M. The internalization route resulting in successful gene expression depends on polyethylenimine both cell line and polyplex type. Mol Ther 2006;14:745–53.
[12] Rejman J, Bragonzi A, Conese M. Role of clathrin- and caveolae-mediated endocytosis in gene transfer mediated by lipo- and polyplexes. Mol Ther 2005;12:468–74.
[13] Midoux P, Breuzard G, Gomez JP, Pichon C. Polymer-based gene delivery: a current review on the uptake and intracellular trafficking of polyplexes. Curr Gene Ther 2008;8:335–52.
[14] Payne CK, Jones SA, Chen C, Zhuang XW. Internalization and trafficking of cell surface proteoglycans and proteoglycan-binding ligands. Traffic 2007; 8:389–401.
[15] Goncalves C, Mennesson E, Fuchs R, Gorvel JP, Midoux P, Pichon C. Macropinocytosis of polyplexes and recycling of plasmid via the clathrin-dependent pathway impair the transfection efficiency of human hepatocarcinoma cells. Mol Ther 2004;10:373–85.
[16] McLendon PM, Fichter KM, Reineke TM. Poly(glycoamidoamine) vehicles promote pDNA uptake through multiple routes and efficient gene expression via caveolae-mediated endocytosis. Mol Pharm; 2010.
[17] Gabrielson NP, Pack DW. Efficient polyethylenimine-mediated gene delivery proceeds via a caveolar pathway in HeLa cells. J Control Release 2009; 136:54–61.
[18] Diaz-Moscoso, Vercauteren D, Rejman J, Benito JM, Ortiz Mellet C, De Smedt SC, et al. Insights in cellular uptake mechanisms of pDNA-polycationic amphiphilic cyclodextrin nanoparticles (CDplexes). J Control Release 2010;143:318–25.
[19] Vercauteren D, Vandenbroucke RE, Jones AT, Rejman J, Demeester J, De Smedt SC, et al. The use of inhibitors to study endocytic pathways of gene carriers: optimization and pitfalls. Mol Ther 2010;18:561–9.
[20] Ivanov Andrei I. Pharmacological inhibition of endocytic pathways: is it specific enough to be useful? Methods Mol Biol 2008;440:15–33.
[21] Strauss O. The retinal pigment epithelium in visual function. Physiol Rev 2005;85:845–81.
[22] Murata T, Cui J, Taba KE, Oh JY, Spee C, Hinton DR, et al. The possibility of gene therapy for the treatment of choroidal neovascularization. Ophthalmology 2000;107:1364–73.
[23] Naik R, Mukhopadhyay A, Ganguli M. Gene delivery to the retina: focus on non-viral approaches. Drug Discov Today 2009;14:306–15.
[24] Lin C, Zhong ZY, Lok MC, Jiang XL, Hennink WE, Feijen J, et al. Novel bioreducible poly(amido amine)s for highly efficient gene delivery. Bioconjug Chem 2007;18:138–45.
[25] Jere D, Arote R, Jiang HL, Kim YK, Cho MH, Cho CS. Bioreducible polymers for efficient gene and siRNA delivery. Biomed Mater 2009;4.
[26] Christensen LV, Chang CW, Kim WJ, Kim SW, Zhong ZY, Lin C, et al. Reducible poly(amido ethylenimine)s designed for triggered intracellular gene delivery. Bioconjug Chem 2006;17:1233–40.
[27] Jeong JH, Kim SH, Christensen LV, Feijen J, Kim SW. Reducible poly(amido ethylenimine)-based gene delivery system for improved nucleus trafficking of plasmid DNA. Bioconjug Chem 2010;21:296–301.
[28] Wang R, Zhou L, Zhou Y, Li G, Zhu X, Gu H, et al. Synthesis and gene delivery of poly(amido amine)s with different branched architecture. Biomacromolecules 2010;11:489–95.
[29] Lin C, Engbersen JFJ. The role of the disulfide group in disulfide-based polymeric gene carriers. Expert Opin Drug Deliv 2009;6:421–39.
[30] Gandhi NS, Mancera RL. The structure of glycosaminoglycans and their interactions with proteins. Chem Biol Drug Des 2008;72:455–82.
[31] Belting M. Heparan sulfate proteoglycan as a plasma membrane carrier. Trends Biochem Sci 2003;28:145–51.
[32] Nakase I, Tadokoro A, Kawabata N, Takeuchi T, Katoh H, Hiramoto K, et al. Interaction of arginine-rich peptides with membrane-associated proteoglycans is crucial for induction of actin organization and macropinocytosis. Biochemistry 2007;46:492–501.
[33] Vives RR, Lortat-Jacob H, Fender P. Heparan sulphate proteoglyeans and viral vectors: ally or foe? Curr Gene Ther 2006;6:35–44.
[34] Mislick KA, Baldeschwieler JD. Evidence for the role of proteoglycans in cation-mediated gene transfer. Proc Natl Acad Sci U S A 1996;93: 12349–54.
[35] Mounkes LC, Zhong W, Cipres-Palacin G, Heath TD, Debs RJ. Proteoglycans mediate cationic Liposome-DNA complex-based gene delivery in vitro and in vivo. J Biol Chem 1998;273:26164–70.

[36] Page E, Goings GE, Upshaw-Earley J, Hanck DA. Endocytosis and uptake of lucifer yellow by cultured atrial myocytes and isolated intact atria from adult rats. Regulation and subcellular localization. Circ Res 1994;75:335–46.
[37] Ernst S, Langer R, Cooney CL, Sasisekharan R. Enzymatic degradation of glycosaminoglycans. Crit Rev Biochem Mol Biol 1995;30:387–444.
[38] Marks DL, Singh RD, Choudhury A, Wheatley CL, Pagano RE. Use of fluorescent sphingolipid analogs to study lipid transport along thepathway endocytic. Methods 2005;36:186–95.
[39] Mercer J, Helenius A. Virus entry by macropinocytosis. Nat Cell Biol 2009; 11:510–20.
[40] Rodal SK, Skretting G, Garred O, Vilhardt F, van Deurs B, Sandvig K. Extraction of cholesterol with methyl-beta-cyclodextrin perturbs formation of clathrin-coated endocytic vesicles. Mol Biol Cell 1999;10:961–74.
[41] Cooper JA. Effects of cytochalasin and phalloidin on actin. J Cell Biol 1987;105:1473–8.
[42] Sampath P, Pollard TD. Effects of cytochalasin, phalloidin, and pH on the elongation of actin-filaments. Biochemistry 1991;30:1973–80.
[43] Peterson JR, Mitchison TJ. Small molecules, big impact: a history of chemical inhibitors and the cytoskeleton. Chem Biol 2002;9:1275–85.
[44] Akinc A, Thomas M, Klibanov AM, Langer R. Exploring polyethylenimine-mediated DNA transfection and the proton sponge hypothesis. J Gene Med 2005;7:657–63.
[45] Bayer N, Schober D, Prchla E, Murphy RF, Blaas D, Fuchs R. Effect of bafilomycin A1 and nocodazole on endocytic transport in HeLa Cells: implications for viral uncoating and infection. J Virol 1998;72:9645–55.
[46] Baravalle G, Schober D, Huber M, Bayer N, Murphy RF, Fuchs R. Transferrin recycling and dextran transport to lysosomes is differentially affected by bafilomycin, nocodazole, and low temperature. Cell Tissue Res 2005; 320:99–113.
[47] Wang LH, Rothberg KG, Anderson RG. Mis-assembly of clathrin lattices on endosomes reveals a regulatory switch for coated pit formation. J Cell Biol 1993;123:1107–17.
[48] Akiyama T, Ishida J, Nakagawa S, Ogawara H, Watanabe S, Itoh N, et al. Genistein, a specific inhibitor of tyrosine-specific protein-kinases. J Biol Chem 1987;262:5592–5.
[49] Praefcke GJK, McMahon HT. The dynamin superfamily: universal membrane tubulation and fission molecules? Nat Rev Mol Cell Biol 2004;5:133–47.
[50] Macia E, Ehrlich M, Massol R, Boucrot E, Brunner C, Kirchhausen T. Dynasore, a cell-permeable inhibitor of dynamin. Dev Cell 2006;10:839–50.
[51] Gschwendt M, Muller HJ, Kielbassa K, Zang R, Kittstein W, Rincke G, et al. Rottlerin, a novel protein kinase inhibitor. Biochem Biophys Res Commun 1994;199:93–8.
[52] Sarkar K, Kruhlak MJ, Erlandsen SL, Shaw S. Selective inhibition by rottlerin of macropinocytosis in monocyte-derived dendritic cells. Immunology 2005;116:513–24.
[53] Romer W, Berland L, Chambon V, Gaus K, Windschiegl B, Tenza D, et al. Shiga toxin induces tubular membrane invaginations for its uptake into cells. Nature 2007;450:670–5.
[54] Liu YW, Surka MC, Schroeter T, Lukiyanchuk V, Schmid SL. Isoform and splice-variant specific functions of dynamin-2 revealed by analysis of conditional knock-out cells. Mol Biol Cell 2008;19:5347–59.
[55] Lakhan SE, Sabharanjak S, De A. Endocytosis of glycosylphosphatidylinositol-anchored proteins. J Biomed Sci 2009;16.
[56] Gong Q, Huntsman C, Ma D. Clathrin-independent internalization and recycling. J Cell Mol Med 2008;12:126–44.
[57] Lundmark R, Doherty GJ, Howes MT, Cortese K, Vallis Y, Parton RG, et al. The GTPase-activating protein GRAF1 regulates the CLIC/GEEC endocytic pathway. Curr Biol 2008;18:1802–8.
[58] Dharmawardhane S, Schurmann A, Sells MA, Chernoff J, Schmid SL, Bokoch GM. Regulation of macropinocytosis by p21-activated kinase-1. Mol Biol Cell 2000;11:3341–52.
[59] Liberali P, Kakkonen E, Turacchio G, Valente C, Spaar A, Perinetti G, et al. The closure of Pak1-dependent macropinosomes requires the phosphorylation of CtBP1/BARS. EMBO J 2008;27:970–81.
[60] Donaldson JG. Arfs, phosphoinositides and membrane traffic. Biochem Soc Trans 2005;33:1276–8.
[61] Frick M, Bright NA, Riento K, Bray A, Merrified C, Nichols BJ. Coassembly of flotillins induces formation of membrane microdomains, membrane curvature, and vesicle budding. Curr Biol 2007;17:1151–6.
[62] Kopatz I, Remy JS, Behr JP. A model for non-viral gene delivery: through syndecan adhesion molecules and powered by actin. J Gene Med 2004;6:769–76.
[63] Paris S, Burlacu A, Durocher Y. Opposing roles of syndecan-1 and syndecan-2 in polyethylenimine-mediated gene delivery. J Biol Chem; 2008:7697–704.
[64] Fan TC, Chang HT, Chen IW, Wang HY, Chang MDT. A heparan sulfate-facilitated and raft-dependent macropinocytosis of eosinophil cationic protein. Traffic 2007;8:1778–95.
[65] Wittrup A, Sandgren S, Lilja J, Bratt C, Gustavsson N, Mörgelin M, et al. Identification of proteins released by mammalian cells that mediate DNA internalization through proteoglycan-dependent macropinocytosis. J Biol Chem 2007;282:27897–904.
[66] Grosse S, Aron Y, Thevenot G, Francois D, Monsigny M, Fajac I. Potocytosis and cellular exit of complexes as cellular pathways for gene delivery by polycations. J Gene Med 2005;7:1275–86.
[67] Khalil IA, Kogure K, Futaki S, Harashima H. High density of octaarginine stimulates macropinocytosis leading to efficient intracellular trafficking for gene expression. J Biol Chem 2006;281:3544–51.
[68] Clement C, Tiwari V, Scanlan PM, Valyi-Nagy T, Yue BYJT, Shukla D. A novel role for phagocytosis-like uptake in herpes simplex virus entry. J Cell Biol 2006;174:1009–21.
[69] Bonazzi M, Spano S, Turacchio G, Cericola C, Valente C, Colanzi A, et al. CtBP3/BARS drives membrane fission in dynamin-independent transport pathways. Nat Cell Biol 2005;7:570–80.
[70] Castellano F, Chavrier P, Caron E. Actin dynamics during phagocytosis. Semin Immunol 2001;13:347–55.
[71] Zhang J, Zhu J, Bu X, Cushion M, Kinane TB, Avraham H, et al. Cdc42 and RhoB activation are required for mannose receptor-mediated phagocytosis by human alveolar macrophages. Mol Biol Cell 2005;16:824–34.
[72] Lambaerts K, Wilcox-Adelman SA, Zimmermann P. The signaling mechanisms of syndecan heparan sulfate proteoglycans. Curr Opin Cell Biol 2009;21:662–9.
[73] Sahay G, Alakhova DY, Kabanov AV. Endocytosis of nanomedicines. J Control Release 2010;145:182–95.
[74] Braeckmans K, Buyens K, Bouquet W, Vervaet C, Joye P, De Vos F, et al. Sizing nanomatter in biological fluids by fluorescence single particle tracking. Nano Lett 2010;10:4435–42.
[75] Säälik P, Padari K, Niinep A, Lorents A, Hansen M, Jokitalo E, et al. Protein delivery with transportans is mediated by caveolae rather than flotillin-dependent pathways. Bioconjug Chem 2009;20:877–87.
[76] Vassilieva EV, Ivanov AI, Nusrat A. Flotillin-1 stabilizes caveolin-1 in intestinal epithelial cells. Biochem Biophys Res Commun 2009;379:460–5.
[77] Finnemann SC. Focal adhesion kinase signaling promotes phagocytosis of integrin-bound photoreceptors. EMBO J 2003;22:4143–54.
[78] Zhao MW, Jin ML, He S, Spee C, Ryan SJ, Hinton DR. A distinct integrin-mediated phagocytic pathway for extracellular matrix remodeling by RPE Cells. Invest Ophthalmol Vis Sci 1999;40:2713–23.
[79] Riento K, Frick M, Schafer I, Nichols BJ. Endocytosis of flotillin-1 and flotillin-2 is regulated by Fyn kinase. J Cell Sci 2009;122:912–8.
[80] Hybiske K, Stephens RS. Mechanisms of *Chlamydia trachomatis* entry into nonphagocytic cells. Infect Immun 2007;75:3925–34.
[81] Irschick EU, Haaa G, Geiger M, Singer W, Ritsch-Marte M, Konwalinka G, et al. Phagocytosis of human retinal pigment epithelial cells: evidence of a diurnal rhythm, involvement of the cytoskeleton and interference of antiviral drugs. Ophthalmic Res 2006;38:164–74.